Evaluation of a 32 x 32 InSb CID array

D. Stefanovitch, F. Sibille

Classification
Physics Abstracts
07.62

Evaluation of a 32 × 32 InSb CID array

D. Stefanovitch and F. Sibille (*)

Observatoire de Meudon, 92190 Meudon, France, (*) Observatoire de Lyon, 69230 Saint Genis Laval, France

(*Reçu le 15 décembre 1981, révisé le 11 février 1982, accepté le 15 février 1982*)

Résumé. — On présente les premiers résultats des essais en laboratoire d'une mosaïque de 32 × 32 détecteurs à l'InSb du type CID (Charge Injection Device).
Les essais ont été effectués à des niveaux de température et de rayonnement de fond beaucoup plus bas que ceux prévus par le constructeur, de façon à se rapprocher des conditions d'une utilisation pour des observations astronomiques.

Abstract. — We present the results of a laboratory evaluation of a two dimensional 32 × 32 InSb detector array of the CID type. The tests have been carried out with levels of background and temperature much lower than foreseen by the manufacturer, in order to evaluate the array under the conditions found in astronomical observations.

1. **Introduction.** — The development of CCD [1] or CID [2] arrays of detectors for the visible light has progressed very rapidly during the last few years, mainly because of the well known Silicon technology. More recently, a considerable effort has been undertaken to implement the same kind of devices with infrared sensitive materials like InSb or HgCdTe, using either monolithic or hybrid approach. These devices have been generally developed for military purposes, implying high background flux, moderately low temperature operation, and restricted availability to the scientific community. Nevertheless, General Electric (GE) [3] has made commercially available on the U.S. territory a bidimensional array of 32 × 32 InSb detectors, with CID read out and associated electronics. It is worth noting that most of the work done in the fast growing field of infrared astronomy has been carried out with instruments tending to reach the highest performance in the rather low background environment of a telescope focus but with only one or very few detectors.

The advent of bidimensional arrays with a significant number of pixels will indeed revolutionize I.R. Astronomy. A GE 32 × 32 InSb CID has been purchased by the C.N.R.S. [4] and the C.F.H.T. [5] for astronomical observations and this article presents the preliminary results of a laboratory evaluation of this device made by the authors at Kitt Peak National Observatory. The evaluation was carried out under low background and low temperature conditions, keeping in mind the ultimate goal of astronomical use.

2. **Description of the CID array.** — The GE array is a monolithic CID of InSb material and has a pixel pattern of 32 rows by 32 columns of square elements. The pitch is 71 × 71 μm^2 with an effective collecting area of 58 × 58 μm^2, thus providing an area filling factor of 66%. The InSb chip and the two silicon scanners which operate the row and column addressing are integrated in a 26 pin flatpack (see Fig. 1).

This flatpack and the first stage of preamplification are mounted inside a dewar, and connected by coaxial cables to the control electronics box which works at room temperature (see Fig. 2). The system was delivered as mounted in a small liquid Nitrogen dewar. After a few initial tests, we moved it into a much larger dewar (Infrared Laboratories, model HD-3), suitable for liquid nitrogen or helium, and equipped with an externally driven filter wheel allowing selection of appropriate wavelengths intervals.

Each sensing element is made up of two capacitor plates respectively connected to a row line and a

(1) CCD : Charge Coupled Device.
(2) CID : Charge Injection Device.
(3) General Electric Company, Optoelectronic Systems Operation, Electronic Systems Division, Electronics Park, Syracuse N.Y. 13221 U.S.A.
(4) Centre National de la Recherche Scientifique.
(5) Canada France Hawaï Telescope Corporation.

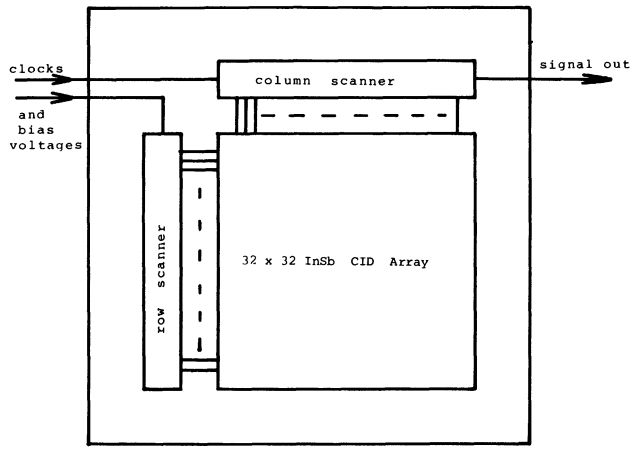

Fig. 1. — Lay-out of the detector array.

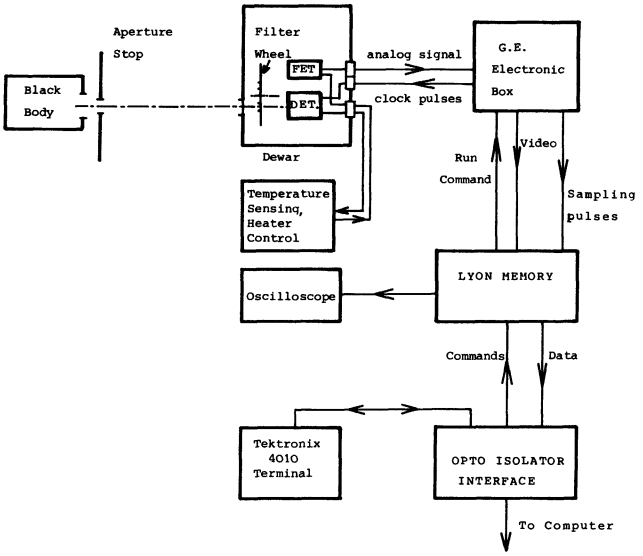

Fig. 2. — Block diagram of the experimental set-up.

column line. These electrodes are biased and create a potential well in which the photon generated charges are confined and accumulate until the well is collapsed. By use of the row and column scanners, one can select a pixel and by applying appropriate voltages to the lines, one can either transfer the charges back and forth between the two plates of that pixel or collapse the potential well, thus injecting the charges into the substrate and creating on the plates a voltage change that can be sensed by a preamplifier. The reader interested in a more detailed explanation is referred to [1] and [2].

Initially, the read out system used the Sequential Row Inject (SRI) mode, in which the 32 columns are sequentially addressed (by the column scanner) and the 32 pixels of every addressed column are read out by the use of the row scanner to sequentially address the 32 rows. In this mode, while a selected pixel was being read out, the 31 other pixels belonging to the same row were being injected (without read out), thus loosing their photon generated charges instead of continuing to integrate up to the time of actual read out. As a result, on every pixel, only the 32nd part of the signal charge was actually sensed (the rest being lost) and the integration time was a little less than the time needed to read out a column. This read out mode provides a good reading performance if one wants to look at bright targets against high background (since it reduces the risk of saturating the device), but makes very inefficient use of the array as an integrating device and is equivalent to having only one 32 pixel column and scanning it accross the image by 32 steps.

The read out scheme has therefore been changed to the more classical Full Frame Integration mode which allows to sequentially inject and read out the 1024 pixels at the end of an integration period taken over the full image, each pixel being injected only once during the read out sequence. In addition, this mode allows to vary the integration time, a requirement that was considered mandatory for astronomical applications.

One classical advantage of CID is the Multiple Non Destructive Read Out (MNDRO) mode which allows to improve the read out S/N ratio as the square root of the number of read cycles [2]. This is not available with the InSb CID, mainly because its transfer efficiency is not as good as that of silicon CID.

3. **Experimental set-up.** — A block diagram of the experimental set-up is shown in figure 2. The detector mount was attached to a brass plate clamped to the cold surface inside the dewar. The same brass plate supported the preamp board (by means of nylon screws and fiber stand-offs) and a cooled optical system comprising :

— an externally driven filter wheel,

— two aperture stops, one very close to the filter wheel and the other close to the dewar's window,

— two radiation shields, one around the detector mount and the other around the filter wheel.

The multiposition filter wheel was equipped with the following filters :

$$\lambda = 2.2\,\mu m \qquad \Delta\lambda = 0.5\,\mu m$$
$$\lambda = 4.7\,\mu m \qquad \Delta\lambda = 0.2\,\mu m\,.$$

A third position was made opaque and was used as a cold shutter.

This optical system provided a low background environment when the 2.2 μm filter was selected. No focusing element was used and the array was operated in the staring mode (no chopping). Outside the dewar, a 500 °C blackbody whose output was controlled by means of calibrated aperture stops was installed at some distance on the optical axis, illuminating the array with a known level of radiation power.

The GE warm electronics comprises a digital board and an analog board. The digital board controls the cold scanners by providing them appropriate clock pulses. Inside the dewar, a cold preamp consists of a FET ([6]) connected in the source follower mode which handles the multiplexed array output and sends it on a low impedance coaxial cable to the analog board, which performs amplification and double correlated sampling and finally outputs a video signal. This video signal is fed to a data acquisition system (built by Lyon Observatory), which digitizes the samples and stores up to 16 consecutive frames in a buffer memory, each frame being made of 1024 12 bit words.

Most of the tests and measurements were carried out by using the equipment in a manual or semi-manual mode, i.e. by looking at the video signal on an oscilloscope, digitizing only the samples coming from a selected pixel, and playing back the memory step by step to access the recorded data. Also a video monitor was used from time to time to get a full image of the array.

Only at the very end of the tests it was possible to connect the experiment to a Varian 620F Computer and to control the CID by means of a very flexible and high performance software initially developed at Kitt Peak for CCD Cameras. This allowed the use of a Tektronix 4010 terminal to assign chosen values to some parameters (i.e. integration time and number of samples to be taken) and to start and control an acquisition run. After completion of a run, the data stored in the buffer memory were transferred into the computer memory, processed, and finally displayed in a practical and flexible way (see Fig. 3).

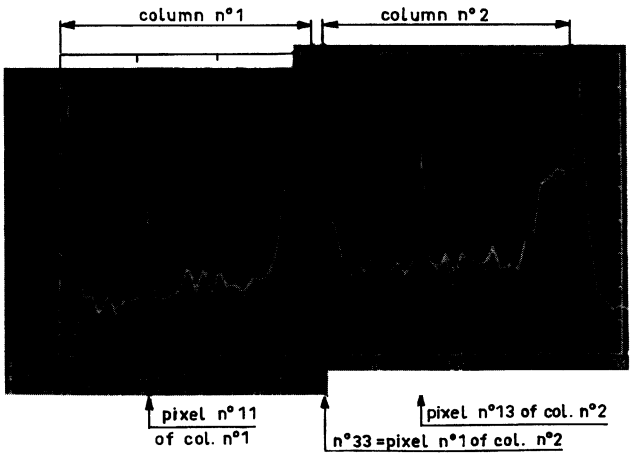

Fig. 3. — Typical display of stored data. The array was read three times and the data were stored in the Lyon memory. Then the data present in the first 70 locations of pages 1, 2 and 3 were displayed and superimposed. One can see column n° 1 en positions 1 through 32 and column n° 2 in positions 33 through 64. Dead pixels n° 11 in col. n° 1 and n° 13 in col. n° 2 can be easily identified by the aid of figure 5. The high plateau at the right hand end of column n° 1 and column n° 2 is an indication that some humidity has been trapped. It will disappear after a good bake-out.

(6) FET : Field Effect Transistor.

4. **Tests and measurements.** — The main points of interest during the tests were dark current, quantum efficiency, saturation level, linearity, read-out noise, fixed pattern noise, and longest possible integration time.

All the tests were performed with the bias levels recommended by the manufacturer, i.e. :

$$V_{\text{row bias}} = V_{\text{column bias}} = -8\,V\,.$$
$$V_{\text{row transfer}} = V_{\text{column transfer}} = -6\,V\,.$$
$$V_{\text{substrate}} = +4.75\,\text{V}\,.$$

4.1 DARK CURRENT. — In the initial SRI read-out mode, the integration time was 125 μs, and all the pixels responded normally to light, except 10 of them which were constantly saturated. As a result of the read-out modification described earlier, the integration time was multiplied by a factor of 32, and even in a low background situation, the array showed complete saturation when operated at liquid nitrogen temperature. Pumping on the nitrogen allowed us to lower the temperature and to see that at about 50 K most of the pixels responded normally to light. Only about thirty of them were still saturated, always with the same pattern, consisting of 5 clusters and a few individuals. Then the array was installed in the large two-fluid dewar, and after a few tests with pumped nitrogen showing the same pattern of 5 clusters (see Fig. 4),

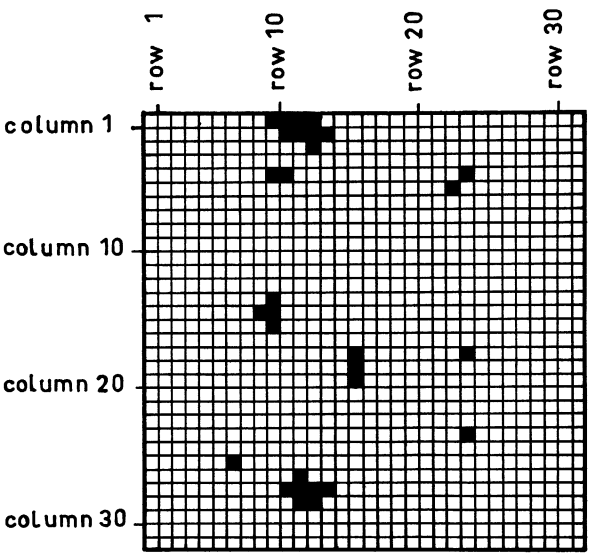

Fig. 4. — Map of saturated pixels at 50 K. (Integration time is 4 ms.)

we went to a lower temperature by the use of liquid helium. At about 20 K, the clusters had disappeared and only 10 individual pixels remained saturated as shown in figure 5. This was considered satisfactory and cooling by helium was adopted as the normal working condition.

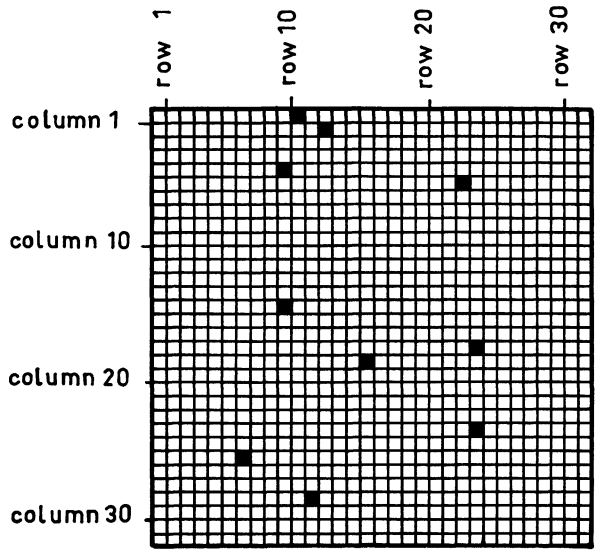

Fig. 5. — Map of saturated pixels at 20 K. (Integration time is 4 ms.)

4.2 LONGEST POSSIBLE INTEGRATION TIME. — Up to that point, the array had been operated in the free-run mode (in other words, it was self scanning at maximum clock speed), but now the modified control electronics also allowed to start individual read-outs by applying trigger pulses at any rate slower than the free run period. Once started, each read-out proceeds at maximum clock speed, then stops when the last column has been read out, and leaves the array integrating, and waiting for the next trigger pulse.

Using an external pulse generator to control the read-out repetition rate, we could increase the integration time to about 200 ms before the array approached saturation (see Fig. 6). At that point, some

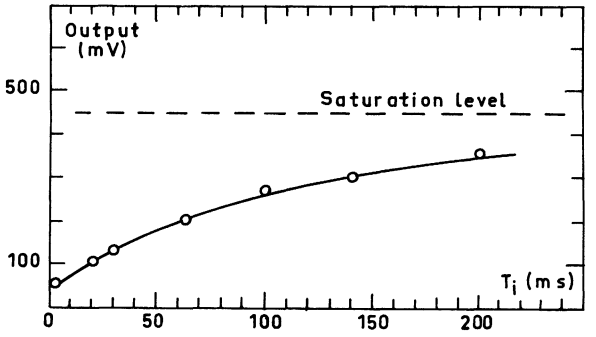

Fig. 6. — Dark current signal *versus* integration time.

light leaks were suspected to dominate over the dark current and this prevented us from doing actual dark current measurements, but nevertheless the tests clearly show that by using helium as a coolant, one can operate the array with integration times much longer than stated by the manufacturer, if a low background environment is provided.

4.3 QUANTUM EFFICIENCY. — To measure the quantum efficiency, a representative pixel was selected, the level of illuminating power was varied by use of the blackbody set up and a plot was made of the output voltage of that pixel *versus* blackbody aperture area (see Fig. 7). The output voltages were referenced to

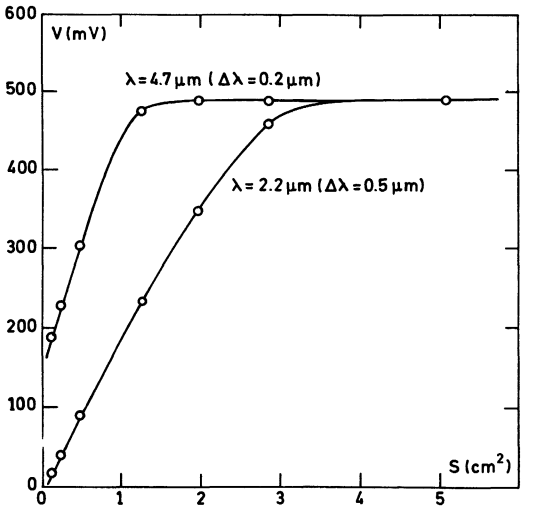

Fig. 7. — Output signal *versus* blackbody aperture area. Output is referenced to level obtained with cold shutter in place. Pixel n° 19 of column n° 1. Integration time : 3 ms. Temperature : 21 K. Gain test : 490 mV for 625 × 10^3 electrons. 500 C blackbody at 1 m.

the value obtained with a cold shutter in place. The slope of the obtained curve at any point of interest is proportional to the responsivity at that point. Knowing the integration time, the amount of energy received through a given narrow filter was easy to compute and then yielded the number of photons received. On the other hand, the amplifier's gain in volts per electrons was determined by use of a built-in test circuit which allowed to inject a precise amount of electrons at the preamplifier's input. The quantum efficiency values obtained by this method are 15% at 2.2 μm and 12% at 4.7 μm and are lower than the manufacturer's measured values almost by a factor of two.

4.4 SATURATION LEVEL. — The saturation level was found to be 600 000 electrons, about one half of the expected value.

4.5 LINEARITY. — Linearity was difficult to test accurately but is certainly not as good as that of visible CID.

4.6 READ-OUT NOISE. — If one uses the GE preamplifier, while cooling with liquid helium, the noise level is about 10 000 electrons r.m.s. This high value is due to the FET being too cold, and it was possible to reduce it to about 3 000 electrons by the use of a heater resistor bonded to the FET's case. Even at a more favourable working temperature, the system is still amplifier noise limited, and the main source of

noise seems to be the capacitive pick-up of scanner clocks. A careful redesign of the wiring inside the dewar should minimize this effect. In addition, the cold FET is in the voltage follower mode (thus having a voltage gain less than unity), while the second stage uses a room-temperature FET of the same type. Some gain is needed in the first stage to improve the overall performance and a cascode scheme would allow this without adding much to the input capacitance.

A poor performance of the sample and hold module on the analog board also added some noise by allowing some spikes to leak through. A second sample and hold module will probably be needed to resample the output of the first one and provide a really clean video signal to the A/D converter inside the Lyon Data Acquisition System.

4.7 FIXED PATTERN NOISE. — A notable FPN exists (about 5% of saturation level from one pixel to the next) and depends loosely on the temperature. It is therefore quite constant from day to day, as long as the working temperature stays about the same. This fixed pattern is not really annoying since one of the first steps taken in the data processing will be to suppress it by substraction of a background or sky image.

5. **Performance of the array.** — The system being amplifier noise limited, the read out noise is independant of the integration time, and the NEP ([7]) for one element of the array is

$$\mathrm{NEP}\,(\lambda, T_i) = \frac{1}{\eta}\,\frac{hc}{\lambda}\,\frac{Ne}{T_i}$$

where λ is the wavelength of the radiation, Ne is the read out noise in r.m.s. electrons at the preamplifier's input, T_i is the actual integration time and η is the quantum efficiency. For the sake of easier comparison, one may convert this NEP to a standard 1 s measuring time NEP (which may require several integrations)

$$\mathrm{NEP}\,(\lambda, 1\ \mathrm{s}) = T_i^{1/2} \times \mathrm{NEP}\,(\lambda, T_i)\,.$$

([7]) NEP : Noise Equivalent Power.

In our case, with the conservative value of $Ne = 10^4$, with η values of 12% and 15% respectively at 4.7 μm and 2.2 μm, and with a 0.1 s integration time, we obtain :

$$\mathrm{NEP}\,(4.7\ \mu\mathrm{m}, 1\ \mathrm{s}) = 1.1 \times 10^{-14}\ \mathrm{W}$$
$$\mathrm{NEP}\,(2.2\ \mu\mathrm{m}, 1\ \mathrm{s}) = 2 \times 10^{-14}\ \mathrm{W}\,.$$

We must again emphasize that these numbers are very conservative, and that a significant improvement is expected from a new design of the preamplifier and from a better temperature control of its cooled transistor. Also a better shielding against stray radiation will allow to increase the integration time, thus improving the NEP (λ, 1 s). It is anticipated that the NEP could go down by a factor of five from the above measured values.

6. **Conclusion.** — This work presents, to the best of our knowledge, the results of the first attempt to use, under low background and below 30 K operation, a large InSb CID array, initially developed for high background and 77 K operation. The main disadvantage of this CID is certainly its poor linearity which puts a severe constraint on the data reduction of photometric measurements.

Nevertheless the NEP figures of about 10^{-14} W (at 4.7 μm) and of 2×10^{-15} W anticipated, in addition to the very large multidetector gain of the array, show that this device is already able to compete with high performance single element InSb detectors. It appears as a modest but extremely promising initial step in the open field of application of large detector arrays to Infrared Astronomy.

Acknowledgments. — This work has been possible thanks to the hospitality of the Infrared Sensor Laboratory at Kitt Peak National Observatory (Tucson, Arizona) and the authors thank F. Gillett, A. Fowler, and P. Britt for their invaluable assistance during the tests.

References

[1] GIBBONS, M. D. *et al.*, *Advances in InSb focal planes, Proceedings of the SPIE.* Vol. **225** (1980). Infrared sensor image technology.

[2] AIKENS, R. S., LYNDS, C. R. and NELSON, R. E., *Astronomical applications of Charge Injection Devices*, SPIE Vol. **78** (1976) Low Light Level Devices.